Low-temperature synthesis of K0.5FeF3 with tunable exchange bias

Qiao-Ru Xu, Yang Liu, Yu-Di Zheng, Wenbin Rui, Yan Sheng et al.

Citation: Appl. Phys. Lett. **103**, 102405 (2013); doi: 10.1063/1.4820476
View online: http://dx.doi.org/10.1063/1.4820476
View Table of Contents: http://apl.aip.org/resource/1/APPLAB/v103/i10
Published by the AIP Publishing LLC.

Low-temperature synthesis of $K_{0.5}FeF_3$ with tunable exchange bias

Qiao-Ru Xu,[1] Yang Liu,[1] Yu-Di Zheng,[1] Wenbin Rui,[2] Yan Sheng,[1] Xuan Shen,[3] Jun Du,[2,a)] Mingxiang Xu,[1] Shuai Dong,[1] Di Wu,[3] and Qingyu Xu[1,a)]
[1]*Department of Physics, Southeast University, Nanjing 211189, China and Key Laboratory of MEMS of the Ministry of Education, Southeast University, Nanjing 210096, China*
[2]*National Laboratory of Solid State Microstructures and Department of Physics, Nanjing University, Nanjing 210093, China*
[3]*Department of Materials Science and Engineering, Nanjing University, Nanjing 210008, China*

(Received 24 March 2013; accepted 7 August 2013; published online 4 September 2013)

Fluorides $K_{0.5}FeF_3$ with tetragonal tungsten bronze structure have been fabricated by solid state reaction at low sintering temperature in the range between 150 °C and 400 °C with the assistance of crystal water during the grinding and sintering processes. Unusual magnetic properties have been observed, including positive exchange bias field (H_E) with negative vertical magnetization shift (M_{shift}), and smaller field cooling (FC) magnetization than the zero field cooling one below 53 K. The results are explained by a core-shell structure consisting of antiferromagnetic core and spin glass (SG) shell with antiferromagnetic interfacial coupling between the pinned interface spins and the SG shell spins. The sign of H_E and M_{shift} can be changed by increasing the cooling field in the FC process, which is attributed to the competition between the antiferromagnetic interfacial coupling and the Zeeman energy of magnetization of the SG shell. © *2013 AIP Publishing LLC*. [http://dx.doi.org/10.1063/1.4820476]

Multiferroic materials possessing at least two of the following orderings (ferro-/antiferromagnetic, ferro-/antiferroelectric, ferroelastic) have attracted many research interests recently due to their abundant physics and potential applications in advanced devices.[1,2] However, multiferroic oxide perovskites are very rare due to that the magnetism and ferroelectricity have the mutual repulsive requirements on the *d* shell electronic configuration, with the former requiring d^n with nonzero *n* and the latter, d^0.[3] In a recent perspective, Scott suggested that more multiferroic materials might be discovered in ferroelectric compounds, which are neither perovskites nor oxides, e.g., fluorides.[4]

Fluorides with tetragonal tungsten bronze (TTB) structure have been considered to be potential multiferroic materials.[4,5] The ferroelectricity in TTB fluorides has been first reported in $K_{0.6}FeF_3$, which has been attributed to the orthorhombic distortion of the TTB cell.[5] Generally, the exchange interaction between the magnetic ions in TTB fluorides is antiferromagnetic (AFM).[6] Previously, the TTB fluorides were synthesized by solid state reaction at high temperatures of above 700 °C, and sealed in mostly platinum tubes due to the strong corrosivity of fluorine.[5–9] In this paper, we report the low-temperature synthesis of $K_{0.5}FeF_3$ at sintering temperature between 150 °C and 400 °C with the assistance of the crystal water, and the detailed studies on the magnetic properties.

Polycrystalline $K_{0.5}FeF_3$ was prepared using appropriate amount of KF, FeF_2, and $FeF_3{\cdot}3H_2O$. All the chemicals are analytical grade. The reagents were first mixed and grinded in the air. Then, the mixture was pressed into pellets and wrapped with a piece of copper foil. After that, they were put in a quartz tube and degassed at 150 °C for 2 h in vacuum ($\sim 10^{-1}$ Pa). Finally, the quartz tube was evacuated in vacuum ($\sim 10^{-4}$ Pa) and sealed with high purity Ar with pressure of 5×10^4 Pa. The sintering process was performed at various temperatures ranging from 150 °C to 710 °C for 24 h. The structure of samples was studied by X-ray diffraction (XRD, Rigaku Smartlab3) using a Cu Kα radiation and transmission electron microscope (TEM, FEI Tecnai G2). The magnetization was measured by PPMS-9 and SQUID-VSM (Quantum Design) from 5 K to 300 K. The *M-H* curves were measured with maximum field of 10 kOe.

Figure 1 shows the experimental XRD patterns for samples synthesized at different temperature, and the standard patterns of $K_{0.5}FeF_3$ (PDF# 24-0861) and $KFeF_3$ (PDF#72-0110). Preliminarily, we can partition the sintering temperatures into two regimes, namely, the low-temperature range (L) of 150 °C–400 °C, and high-temperature range (H) of 500 °C–710 °C. In regime L, the main phase of $K_{0.5}FeF_3$ has already been generated even at the lowest sintering temperature of 150 °C,[10] except for several small miscellaneous diffraction peaks. The mechanism has been confirmed to be due to the assistance of the crystal water in reagent $FeF_3{\cdot}3H_2O$.[10] In regime H, the results we got are quite different from other reports.[5,8] Above the certain sintering temperature of 500 °C, $K_{0.5}FeF_3$ cannot be obtained by our method. Instead, $KFeF_3$ becomes the main phase, including some other impurity phases. We sealed FeF_3 in a quartz tube and sintered at 710 °C. Only FeF_2 and some other impurities were left and no FeF_3 can be found. The transition of Fe^{3+} to Fe^{2+} at high temperature might account for the formation of $KFeF_3$. XRD results suggest that the quality of the sample sintered at 230 °C is the best; we select it for the following detailed structural and magnetic characterizations.

The TEM image shown in Fig. 2(a) reveals the average particle size of about 20 nm, indicating the high surface-to-volume ratio. The small particle size is due to the low

a)Authors to whom correspondence should be addressed. Electronic addresses: jdu@nju.edu.cn and xuqingyu@seu.edu.cn

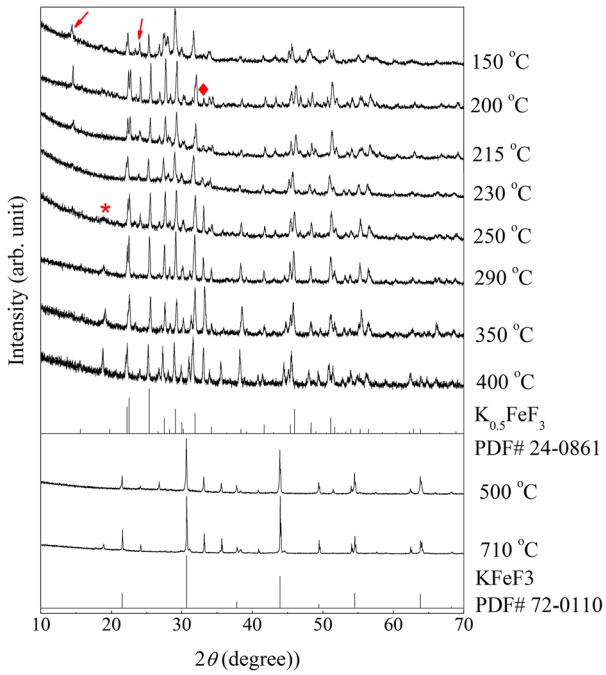

FIG. 1. XRD patterns for the samples sintered at various temperatures. The symbols mark the impurity phases.

sintering temperature, which will provide abundant surface. The high resolution TEM (HRTEM) image shown in Fig. 2(b) indicates the irregular shape of the particles. The high content of irregular surface of particles possibly makes the AFM exchange interaction in the bulk much complicated, leading to the sophisticated magnetic phenomena, such as spin glass (SG) behavior, diluted AFM behavior, etc.[11,12]

Figure 3(a) shows the zero field cooling (ZFC) and field cooling (FC) *M-T* curves, which were measured under 1000 Oe with increasing temperature from 5 K to 300 K and cooling field (H_{cool}) of 1000 Oe for FC curve. The ZFC magnetization bifurcates from the FC process at 137 K with peak position at 130 K. The Curie-Weiss law was used to fit the data of $1/M_{FC}$ above 150 K, as indicated by the dashed line in the inset. The extrapolated Curie-Weiss temperature Θ is ∼−492 K, indicating the AFM structure. Thus, a paramagnetic to AFM transition takes place at the Néel temperature (T_N) of 130 K. T_N is quite close to the reported ones of other TTB fluorides, such as $K_{0.6}FeFe_3$ (122 K),[7] $KMn_{1-x}Co_xFeF_6$ (110 K-150 K),[9] etc. The relatively large value of $|\Theta|/T_N > 3$ indicates the frustrated magnetic behavior, which results from the competition among the AFM exchange interactions

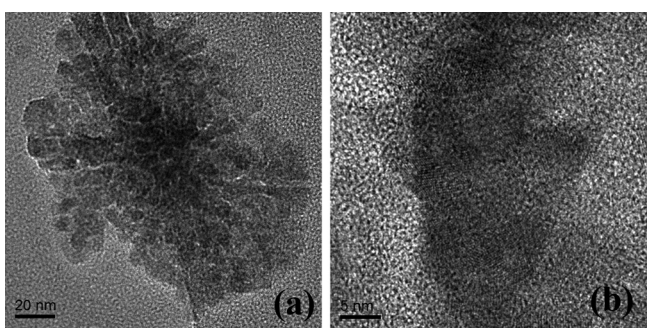

FIG. 2. (a) TEM image of $K_{0.5}FeF_3$ particles. (b) HRTEM image of one particle.

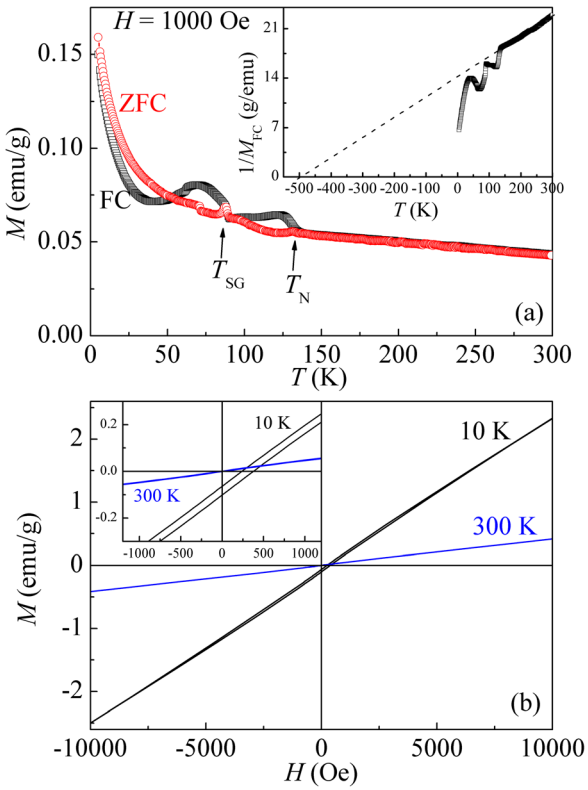

FIG. 3. (a) The ZFC and FC *M-T* curves. The inset shows the corresponding $1/M_{FC}$ vs. *T* with linear fitting for the high temperature paramagnetic part. (b) The *M-H* curves measured at 10 K and 300 K. The inset shows the enlarged view.

of magnetic ions at the triangle sites in the TTB structure.[13] When the sample is further cooled down to T_{SG}–87 K, a second magnetic phase transition can be seen in the FC curve, with a sharp peak in the ZFC curve. This is a typical indication of the SG behavior at low temperature,[14–16] which was further confirmed by the dc magnetic relaxation measurement at 10 K.[10] The SG behavior has been often observed in the surface of AFM nanoparticles, such as $SrMn_3O_{6-\delta}$,[17] CuO,[18] etc. This can be attributed to the frozen uncompensated surface spins in the nanoparticles.[18] Interestingly, a cross point of FC and ZFC *M-T* curves can be seen at 53 K, below which the FC magnetization is smaller than the ZFC magnetization. Similar phenomenon has been observed in Sr_2YbRuO_6, which has been interpreted by the AFM interaction between the different ferromagnetic (FM) components.[19]

M-H curve measured at 10 K (Fig. 3(b)) with maximum field of 10 kOe after 1000 Oe field cooling shows not only the positive exchange bias field (H_{eb}), but also the negative vertical magnetization shift (M_{shift}). H_{eb} is 308 Oe, which is defined as $H_{eb} = (H_{c1} + H_{c2})/2$, where H_{c1} and H_{c2} are the left and right coercive fields, respectively. M_{shift} is −0.083 emu/g, which is defined as $M_{shift} = (M_+ + M_-)/2$, where M_+ and M_- are the positive and negative remnant magnetization, respectively.[20] Such phenomenon was often observed in the AFM/SG core/shell system with negative H_{eb} and positive M_{shift}.[17,18,21–23] Positive H_{eb} has been observed in the Fe-film/CoO-nanoparticle system, which has been interpreted by AFM exchange coupling between the FM layer and the SG layer.[24] Furthermore, negative M_{shift} also indicates AFM interfacial coupling.[18,25]

Fig. 4(a) shows the temperature dependence of H_c and H_{eb}. Positive H_{eb} was observed below 95 K (compensation temperature, T_0, at which H_{eb} changes sign) with maximum value of 531 Oe at 35 K. With further increasing temperature to the T_N of 130 K, negative H_{eb} was observed with maximum value of −229 Oe at 120 K. M_{shift} shows the similar temperature dependence as that of H_{eb}. However, H_c can only be observed below 105 K with similar temperature dependence to that of H_{eb}. The sign change of H_{eb} with increasing temperature has also been observed in the FM/SG heterostructures,[26,27] which is interpreted by the interaction between the FM spins, interface spins and SG bulk spins. Here, we adopt this idea and propose a model to explain the evolution of the exchange bias behavior, as indicated by the scheme in Fig. 4(b). We neglect the induced paramagnetic moment of the AFM core above T_N and SG shell above T_{SG}. H_{eb} and M_{shift} display the similar trend with variation of temperature, indicating that H_{eb} and M_{shift} are closely correlated with each other and have the same origin. M_{shift} has been ascribed to the pinned spins at the interface,[28] providing a microscopic torque on the neighboring spins. As a result, the magnetic hysteresis loop shifts horizontally, and H_{eb} appears consequently. With decreasing temperature through T_N, the interface spins between the AFM core and SG shell were aligned to the direction of H_{cool}, and pinned by the AFM core. This is a normal exchange bias effect, leading to negative H_{eb} and positive M_{shift}. With further decreasing temperature through the T_{SG}, the spins in the SG shell will be frozen, and aligned antiparallel to the direction of H_{cool} due to the interfacial AFM coupling with the interface spins. Therefore, H_{eb} gradually changes its sign from negative to positive through T_0, which is very close to T_{SG}. The frozen spins in SG shell at interface were pinned antiparallel to H_{cool}, leading to negative M_{shift}. With further decreasing temperature, more spins of the SG shell were forced to be aligned antiparallel to H_{cool}, leading to the smaller FC magnetization than the ZFC magnetization below 53 K.

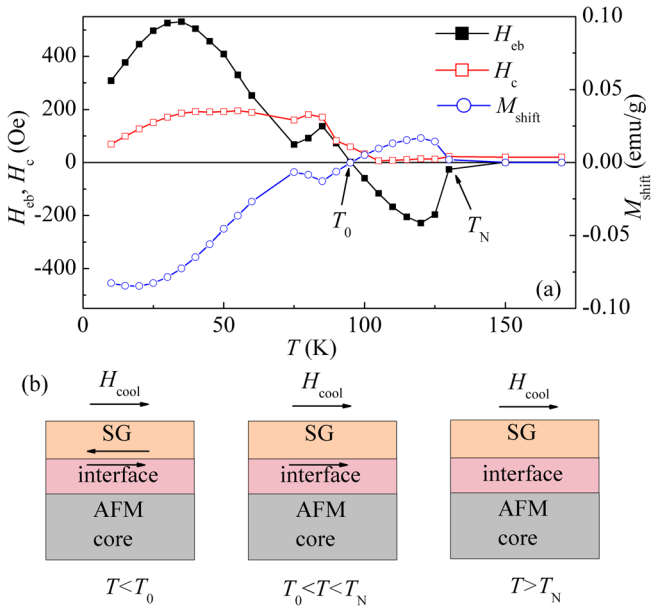

FIG. 4. (a) Temperature dependence of the H_{eb}, H_c, and M_{shift}. (b) Scheme of the spin structure of the AFM core/SG shell model in various temperature ranges.

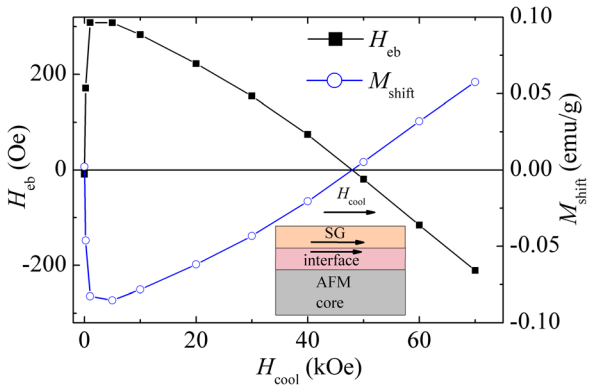

FIG. 5. The cooling field dependence of H_{eb} and M_{shift} at 10 K. The inset shows the spin structure of sample under cooling field larger than 48 kOe using the AFM core/SG shell model.

The signs of H_{eb} and M_{shift} can be changed not only by the temperature, but also by the magnitude of H_{cool} in the FC process. We cooled the sample from temperature above the T_N with different values of H_{cool} to 10 K. As shown in Fig. 5, the absolute values of H_{eb} and M_{shift} increase abruptly with increasing field to 1000 Oe, which can be understood by the alignment of the interface spins and the SG shell spins. The maximum absolute values of H_{eb} and M_{shift} might be achieved between 1000 Oe and 5000 Oe. With further increasing H_{cool}, the absolute values of H_{eb} and M_{shift} both decrease with increasing H_{cool}, and finally both signs were changed at H_{cool} of about 48 kOe. This can be understood by the increase of the Zeeman energy of the spins in SG shell with increasing H_{cool}, which overcomes the interfacial AFM coupling and more and more spins are aligned to the direction of H_{cool}. As shown by the sketched model in the inset of Fig. 5, with increasing the strength of H_{cool}, the net spins in SG shell were aligned to be parallel to H_{cool}, leading to negative H_{eb} and positive M_{shift} simultaneously.

In conclusion, $K_{0.5}FeF_3$ have been fabricated by solid state reaction at low sintering temperature in the range between 150 °C and 400 °C with the assistance of crystal water during the grinding and sintering process. Unusual positive H_E with negative M_{shift} has been observed at 10 K. Furthermore, the FC magnetization is smaller than the ZFC magnetization at temperature below 53 K. The results have been explained by the AFM core/SG shell structure with AFM interfacial coupling between the interface spins and the SG shell spins. The sign of exchange bias field and magnetization shift can be reversed by increasing H_{cool}, which has been attributed to the competition between the interfacial AFM coupling and the Zeeman energy of the magnetization of SG shell.

This work was supported by the State Key Programme for Basic Research of China (2010CB923401 and 2010CB923404), the National Natural Science Foundation of China (51172044, 11074112, 11004027, and 11174131), the Natural Science Foundation of Jiangsu Province of China (BK2011617), the 333 project of Jiangsu province, the Scientific Research Foundation for the Returned Overseas Chinese Scholars, State Education Ministry, and the Student Research Training Program of Southeast University (No. 111028621).

[1]W. Eerenstein, N. D. Mathur, and J. F. Scott, Nature **442**, 759 (2006).
[2]K. F. Wang, J.-M. Liu, and Z. F. Ren, Adv. Phys. **58**, 321 (2009).
[3]N. A. Hill, J. Phys. Chem. B **104**, 6694 (2000).
[4]J. F. Scott and R. Blinc, J. Phys.: Condens. Matter **23**, 113202 (2011).
[5]F. Mezzadri, S. Fabbrici, E. Montanari, L. Righi, G. Calestani, E. Gilioli, F. Bolzoni, and A. Migliori, Phys. Rev. B **78**, 064111 (2008), and references therein.
[6]E. Banks, M. Shone, R. F. Williamson, and W. O. J. Boo, Inorg. Chem. **22**, 3339 (1983).
[7]R. Blinc, G. Tavčar, B. Žemva, D. Hanžel, P. Cevc, C. Filipič, A. Levstik, Z. Jagličič, Z. Trontelj, N. Dalal, V. Ramachandran, S. Nellutla, and J. F. Scott, J. Appl. Phys. **103**, 074114 (2008).
[8]Sk. Mohammad Yusuf, L. Madhav Rao, R. Mukhopadhyay, S. Giri, K. Ghoshray, and A. Ghoshray, Solid State Commun. **101**, 145 (1997).
[9]S. Giri and K. Ghoshray, Phys. Rev. B **57**, 5918 (1998).
[10]See supplementary material at http://dx.doi.org/10.1063/1.4820476 for the analysis of the XRD pattern of $K_{0.5}FeF_3$ prepared at 150 °C, the preparation with and without crystal water, and the dc magnetic relaxation measurement.
[11]L. Chen, Y. Yang, and X. Meng, Appl. Phys. Lett. **102**, 203102 (2013).
[12]P. K. Manna, S. M. Yusuf, R. Shukla, and A. K. Tyagi, Appl. Phys. Lett. **96**, 242508 (2010).
[13]S. Giri, K. Ghoshray, and A. Ghoshray, Solid State Commun. **93**, 493 (1995).
[14]B. Song, J. Jian, H. Bao, M. Lei, H. Li, G. Wang, Y. Xu, and X. Chen, Appl. Phys. Lett. **92**, 192511 (2008).
[15]S. Dhar, O. Brandt, A. Trampert, K. J. Friedland, Y. J. Sun, and K. H. Ploog, Phys. Rev. B **67**, 165205 (2003).
[16]B. Antic, G. F. Goya, H. R. Rechenberg, V. Kusigerski, N. Jovic, and M. Mitric, J. Phys.: Condens. Matter **16**, 651 (2004).
[17]J. Y. Yu, S. L. Tang, X. K. Zhang, L. Zhai, Y. G. Shi, Y. Deng, and Y. W. Du, Appl. Phys. Lett. **94**, 182506 (2009).
[18]C. Díaz-Guerra, M. Vila, and J. Piqueras, Appl. Phys. Lett. **96**, 193105 (2010).
[19]R. P. Singh and C. V. Tomy, J. Phys.: Condens. Matter. **20**, 235209 (2008).
[20]A. A. Belik, Inorg. Chem. **52**, 2015 (2013).
[21]S. Karmakar, S. Taran, E. Bose, B. K. Chardhuri, C. P. Sun, C. L. Huang, and H. D. Yang, Phys. Rev. B **77**, 144409 (2008).
[22]H. Duan, S. Yuan, X. Zheng, and Z. Tian, Chin. Phys. B **21**, 078101 (2012).
[23]S. K. Giri, A. Poddar, and T. K. Nath, J. Appl. Phys. **112**, 113903 (2012).
[24]W. Zhang, T. Wen, and K. M. Krishnan, Appl. Phys. Lett. **101**, 132401 (2012).
[25]J. Nogués, C. Leighton, and I. K. Schuller, Phys. Rev. B **61**, 1315 (2000).
[26]M. Ali, P. Adie, C. H. Marrow, D. Greig, B. J. Hickey, and R. L. Stamps, Nature Mater. **6**, 70 (2007).
[27]F. Yuan, J. Lin, Y. D. Yao, and S. Lee, Appl. Phys. Lett. **96**, 162502 (2010).
[28]X. H. Huang, J. F. Ding, G. Q. Zhang, Y. Hou, Y. P. Yao, and X. G. Li, Phys. Rev. B **78**, 224408 (2008).